2023 temperatures reflect steady global warming and internal sea surface temperature variability

Check for updates

Bjørn H. Samset [1] ✉, Marianne T. Lund [1], Jan S. Fuglestvedt [1] & Laura J. Wilcox [2]

2023 was the warmest year on record, influenced by multiple warm ocean basins. This has prompted speculation of an acceleration in surface warming, or a stronger than expected influence from loss of aerosol induced cooling. Here we use a recent Green's function-based method to quantify the influence of sea surface temperature patterns on the 2023 global temperature anomaly, and compare them to previous record warm years. We show that the strong deviation from recent warming trends is consistent with previously observed sea surface temperature influences, and regional forcing. This indicates that internal variability was a strong contributor to the exceptional 2023 temperature evolution, in combination with steady anthropogenic global warming.

Anthropogenic global warming, driven primarily by emissions of greenhouse gases, has progressed at a broadly steady rate of around 0.2 °C/decade since at least 1970[1]. Recently, however, several studies have also documented a minor step-up in the rate of global mean surface temperature anomaly (GSTA) increase around 1990[2–4], a continued rise in the global energy imbalance[5], and an acceleration in the accumulation of ocean heat content[6]. Factors suggested to have driven this increase include continued greenhouse gas buildup from anthropogenic emissions, and loss of cooling from anthropogenic aerosols after sulfur emissions cleanup[7], notably in China and in the global shipping sector.

Despite this apparent increase in warming rates and a transition of the Equatorial Pacific into an ENSO-positive state, the record surface temperature anomalies recorded through 2023 came as a surprise. All major temperature series show 2023 as the warmest year on record. The margin by which the record was set, around 0.15 °C, was also unusual, but not unprecedented for strong El Niño years. Notably, however, several ocean basins saw unprecedented surface temperatures through much of the year, including the Equatorial and North Pacific, the North Atlantic, and the Southern Ocean[8,9].

A core question is whether this strong anomaly is consistent with internal variability[10] and known decadal scale regional climate forcing, or if it indicates a rapid change in the climate system – or our influence on it[4,11]. The cleanup of shipping emissions has been implicated[12], as has the 2021 Hunga Tonga volcano[13], and a possible aerosol-related unmasking of a stronger-than-expected climate sensitivity. The possibility however remains that the 2023 GSTA record was simply a combination of ongoing anthropogenic influences, together with a sea surface temperature pattern that is within the ranges of observed interannual and decadal variability.

Here, we investigate this question using a recently introduced method that can isolate the contribution to the monthly or annual GSTA from the pattern of sea surface temperatures (SSTs)[3,14]. SST anomalies in different geographical locations are known to have varying influences on global temperatures, the so-called pattern effect[15]. Many studies have shown that this influence can be consistently quantified in Earth System Models, e.g. using simulations that independently perturb SSTs in multiple locations (Green's functions)[16–18]. Our approach is to utilize a Green's function (based on NCAR CESM1; see "Methods" section) to quantify the component of interannual (or monthly) GSTA variability that arises from the different ocean basins using time series of observed surface temperatures, i.e. the SST pattern after the pattern of global warming has been removed with gridpoint-by-gridpoint detrending[14]. The method makes no assumptions about the causes of SST trends or variability. It therefore lets us compare the SST pattern-induced corrections for a given year to previous observed years, regardless of whether that pattern is forced or natural, and therefore determine if the net influence is unprecedented or still within the bounds of previous observations. Note that the results will depend on the detailed response of the CESM1 model to localized SST perturbations, however, other studies have shown that the general spatial pattern and atmospheric dynamical features of such Green's functions are broadly similar between models[16,18–20].

Results

A common question is whether the 2023 Global Surface Temperature Anomaly (GSTA) was record-breaking by a record margin. In Fig. 1, we test this by calculating the margin for each record-breaking year, for four major temperature reconstructions (HadCRUT5, NOAA, Berkeley

[1]CICERO Center for International Climate Research, Oslo, Norway. [2]National Centre for Atmospheric Science, Department of Meteorology, University of Reading, Reading, UK. ✉e-mail: b.h.samset@cicero.oslo.no
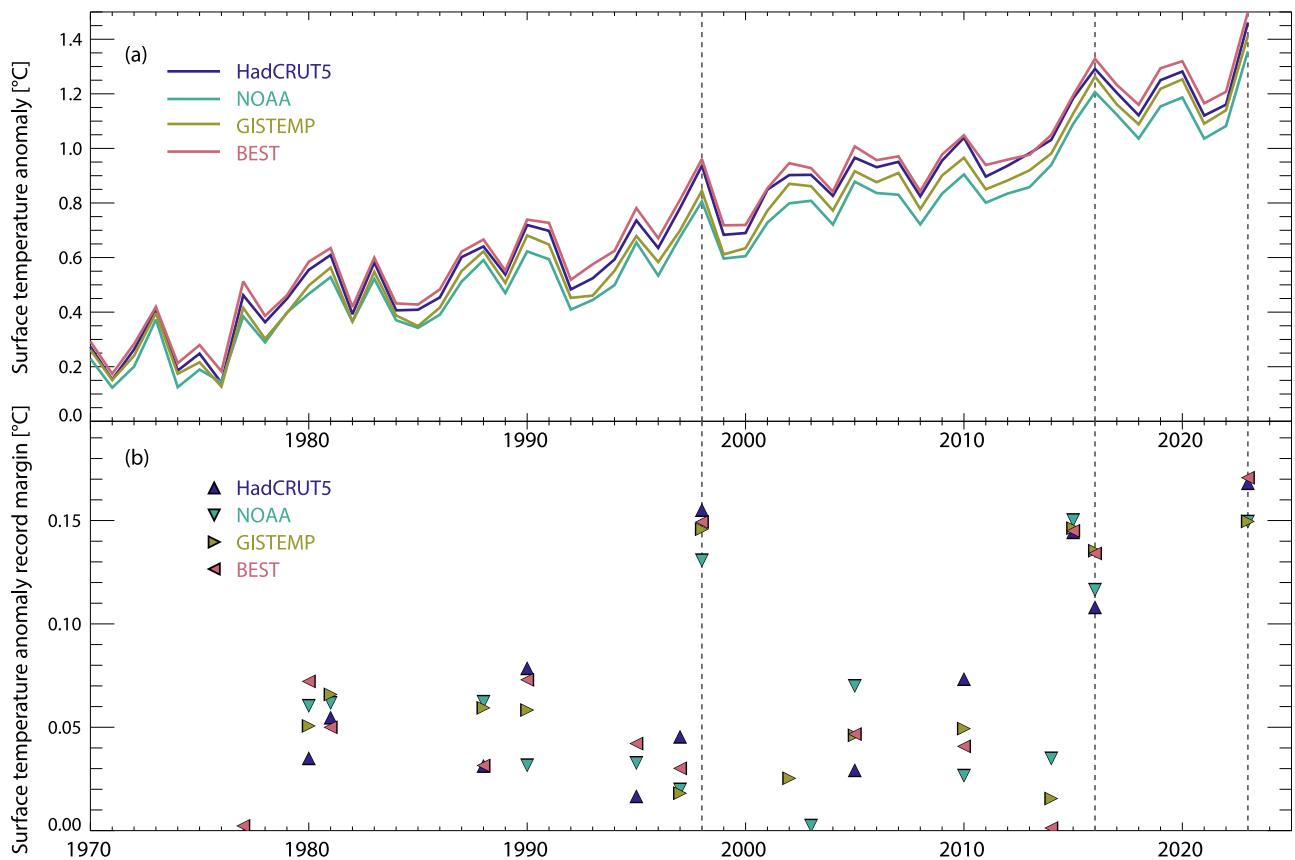
Fig. 1 | Surface temperature anomalies and record margins since 1970. a Annual mean global surface temperature anomalies (GSTA), for four data series, relative to 1850–1900 (1880–1900 for GISTEMP). **b** Annual mean surface temperature record margins (increase over the previously highest recorded value). Dashed lines indicate El Niño dominated years (1998, 2016, 2023).

Earth, and GISTEMP). Most GSTA records since 1970 were set by margins of around 0.05 °C, while in El Niño years, margins of up to 0.15 °C have been recorded. Results are very similar for the four reconstructions. For 2023, the margins were indeed record high (0.17 °C) in two series (HadCRUT5 and BEST), while for the others it was on par with other recent El Niño years. This is consistent with expectations for a situation of strong but steady global warming, modulated by (ENSO-dominated) internal variability. From the observations over the last 50 years, there is therefore no immediate cause to claim that record margins are changing with time, which is, in turn, consistent with a broadly steady rate of global surface warming.

We now investigate the overall SST pattern influence on 2023 global mean temperatures. Figure 2a shows the annual and monthly mean, pattern corrected, GSTA for the last 10 years, with the monthly SST-induced correction factor highlighted as red for anomalously warm (red) or cool (blue) months.

After corrections, 2023 is still the warmest year on record. Now, however, it falls in line with recent long-term warming trends[2,3]. As expected for an El Niño dominated year, 2023 had a stronger-than-usual warm influence from sea surface temperatures throughout most of the year, following on from a series of relatively cool months influenced by multi-year La Nina conditions. However, there was a similar 12-month period of strong SST pattern-induced corrections around the last major El Niño episode, in 2015/2016. Taking the observational record (HadCRUT5[21]; using 1950–2023 to ensure near-global coverage of ocean temperatures), we find that the monthly corrections through 2023 are well within the historical spread (Fig. 2e). In fact, when we select the four other years with strongest SST-induced corrections (1952, 1969, 1998, 2016), their distributions of monthly corrections,

as well as their overall annual corrections, are very similar to 2023. The same is true for global mean corrections (Fig. 2f). We do find that, for HadCRUT5, 2023 is the year on record with the strongest SST-induced GSTA corrections, but with a small margin relative to the years mentioned. Compared to an ensemble of CMIP6 models, the 2023 correction is in the upper 5th percentile, but not exceptional. Note that for some models, we use multiple ensemble members to further sample the effects of internal variability. The overall conclusions are not influenced by this.

A natural question is whether the result is dependent on the temperature reconstruction of HadCRUT5. To test this, we have performed similar analyses for three other series (NOAA, Berkeley Earth, and GISTEMP). While there are minor differences in the ranking of years, all four series identify the same "strongest correction" years. All support the conclusion that 2023 had a strong contribution to its temperature anomaly from the SST pattern, but not an unprecedented one. See Supplementary Figs. 1–3.

To put the 2023 temperatures in a wider context, Fig. 3 shows an update of the analysis of the recent rate of global surface warming presented in Samset et al.[3]. After Green's function-based filtering, we find warming rates (in HadCRUT5) for the recent 10 (2014–2023), 20 (2004–2023) and 50 (1974–2023) years of 0.29, 0.27, 0.19 °C/decade, respectively.

Finally, we investigate where the SST corrections come from, geographically, and whether the 2023 pattern of SST corrections is also consistent with what has previously been observed. Figure 4 compares 2023 to the four examples, strong correction, and years. The maps show the product of Green's function and the observed SST pattern, such that the total correction (globally or regionally) is the sum of all relevant grid boxes.
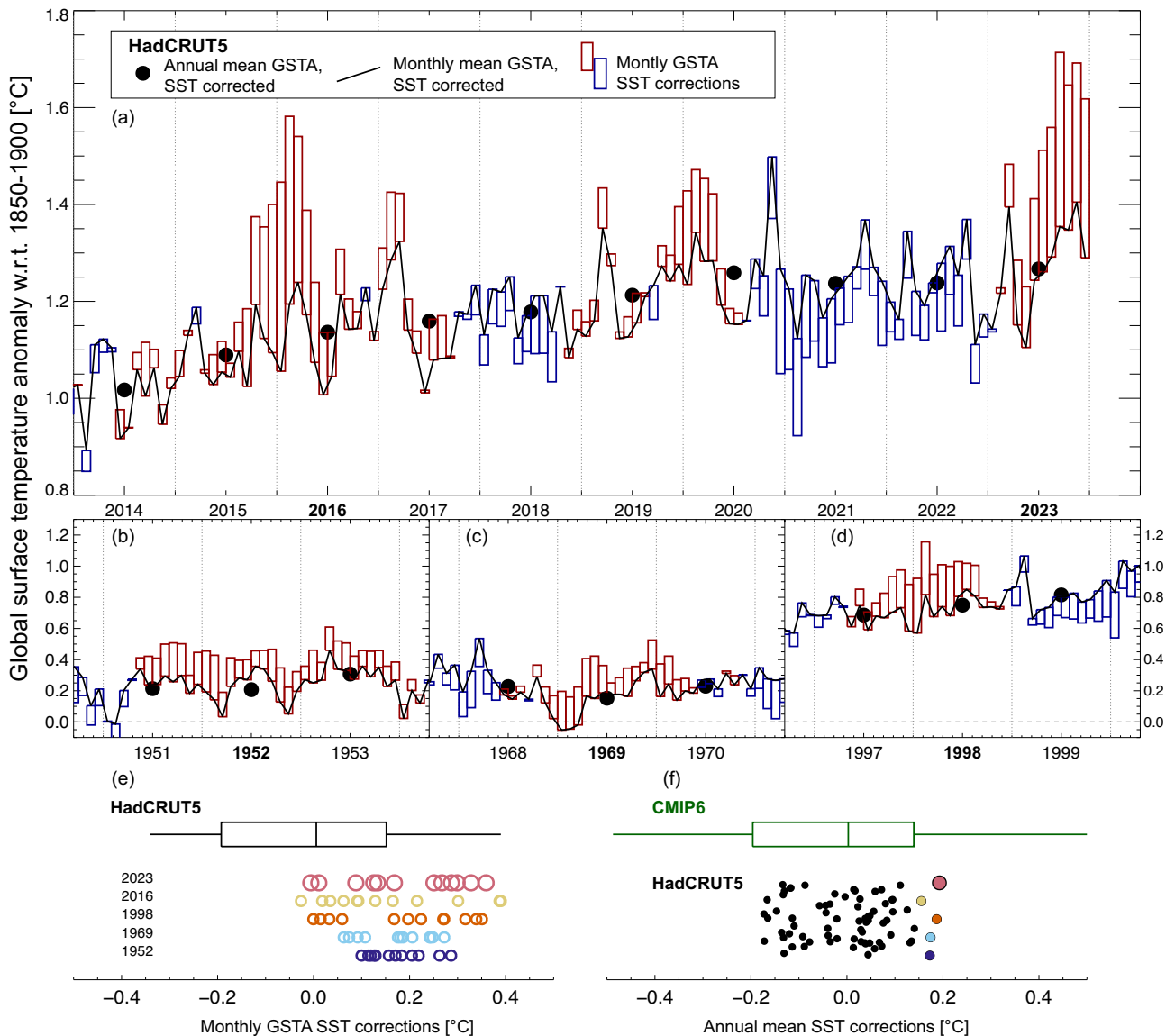
Fig. 2 | Recent global mean surface temperature anomaly evolution in Had-CRUT5. a Annual means, and corrections from the SST pattern quantified via a Green's Function. 2023 and 2016 stand out as having notably strong positive SST pattern corrections. **b–d** Similar, for previous strong SST correction years (1952, 1969, 1998). **e** Monthly correction factors, for 1950–2023 (box-and-whisker) and the selected strong correction years. The box shows the 5–95% range, and the whiskers show the max/min range. **f** Annual correction factors, for CMIP6 (box-and-whisker), and HadCRUT5 (1950–2023). Strong correction years are shown in colours.

Overall, we find very similar patterns between strong correction years, but with notable differences in some ocean basins. All five years were clearly influenced by El Niño conditions in the Equatorial Pacific, and have anomalously warm Tropical North Atlantic conditions. Elsewhere, the influence varies between years. Separating the global corrections by major ocean basins, we find that 2023 was consistent with both observed and modelled variability (Fig. 2b). The most notable outlier is in the Southern Ocean, however here the observational datasets have incomplete coverage for some of the selected years so we place less weight on this result. The North Atlantic also made very strong contributions to GSTA in 2023. For the Tropical North Atlantic (0–30 N) it was the strongest on record, but further north it was still in line with previous observations.

Discussion

The very strong deviation of the 2023 GSTA from recent global warming trends is therefore broadly attributable to the warm state of the various ocean basins. Independently, however, none of the basins had conditions

that were markedly anomalous, or outside the range simulated for the historical era (1850–2014) by recent Earth System Models. What was special about 2023 was rather that multiple ocean basins had warm anomalies at the same time. Hence, it is possible that the 2023 record temperature, rather than heralding an acceleration in surface warming, was consistent with a combination of steady, anthropogenic global warming and ocean surface temperature variability on interannual and decadal scales. Previous years with comparable anomalies, and SST patterns, include 1953, 1969, 1998 and 2016, in all four observational series studied.

We note, however, that our method does not identify the underlying reasons behind the 2023 SST pattern, or for those in earlier years. A shift in global warming induced e.g. by an upwelling of previously stored deeper water temperatures, or factors such as the global energy imbalance, aerosol cleanup or changes in cloudiness anomalously affecting some ocean basins, would also produce SST-induced corrections in our analysis, and could therefore still have contributed to 2023 temperatures. The transition
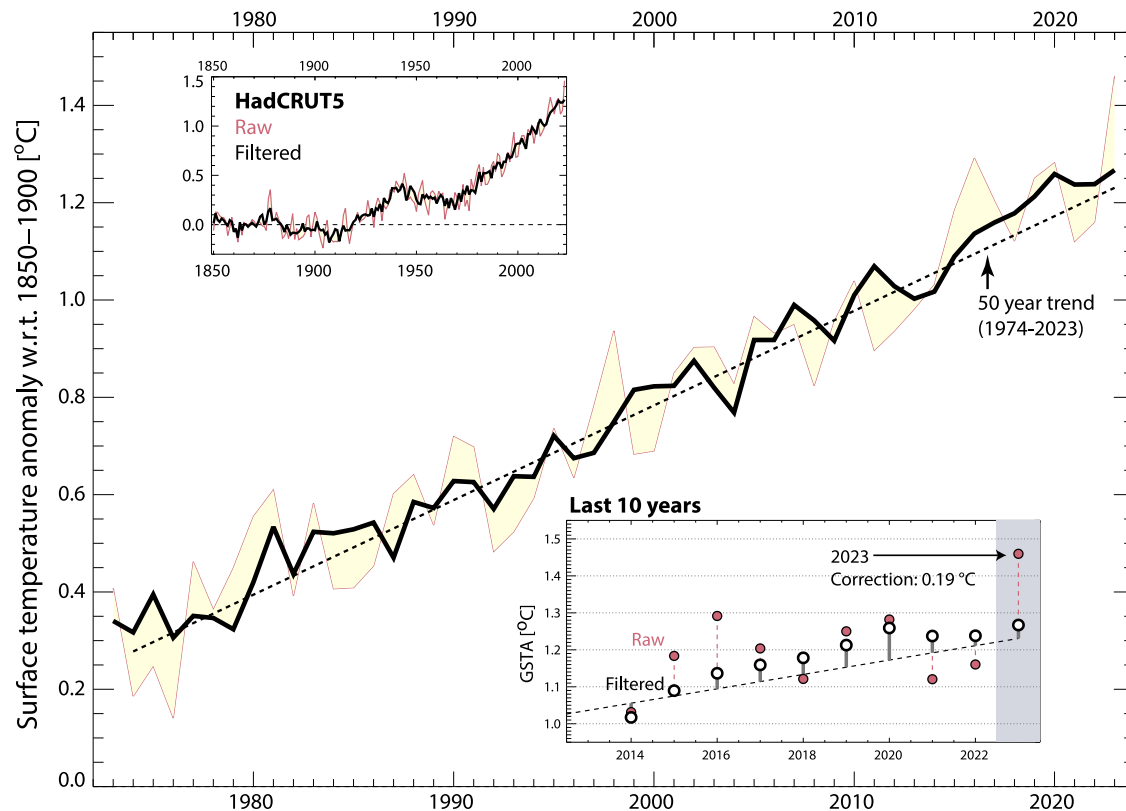
Fig. 3 | 50 years of global surface warming. All panels show global, annual mean surface temperature anomalies from the HadCRUT5 data series, raw (red) and SST influence filtered via a model-derived transfer function (black). The upper and lower insets show, respectively, the full data series since 1850, and the latest 10 years. Anomalies are taken relative to 1850–1900. The dashed black line shows the 50-year trend (0.19 °C/decade). Update from Samset et al.[3].

to El Niño conditions after a multi-year La Nina event is also rare in the observed climate history, making 2023 special also for this reason. Other studies have recently investigated the role of pacific temperatures for the 2023 GSTA, reaching seemingly differing conclusions[11,22]. Our study indicates a marked role of El Niño through the latter part of 2023, consistent with Forster et al.[22].

Further investigations into the causes of the recent very strong surface warming are clearly warranted, notably including analyses of upper ocean heat uptake in various basins, and the regional influences of aerosol emissions changes. 2023 set record temperatures and had sea-surface temperatures in most ocean basins that were unprecedented in the observed records. However, 2023 was not necessarily a harbinger of rapid near-term surface warming, beyond the high global warming rates already known to result from anthropogenic emissions of greenhouse gases and aerosols.

Methods

The methods used in this study build on an approach pioneered and utilized in two previous publications[3,14]. We here explain the main elements and refer to the previous studies for further documentation and validation.

Datasets

The primary dataset used in this study is the HadCRUT5 gridded dataset of global historical surface temperature anomalies, version 5.0.2.0[21]. We used monthly data for the period January 1850–December 2023.

For consistency checking, we also used three other gridded surface temperature data products, on monthly resolution, from their start dates and through December 2023: The GISS Surface Temperature Analysis version 4 (GISTEMP v4)[23,24], NOAA Global Surface Temperature Dataset (NOAAGlobalTemp) Version 5.1 (updated July 2023), and Berkeley Earth (March 2024 update)[25].

Trend removal

The pattern of monthly internal temperature variability is isolated from the long-term influence of anthropogenic warming via a boxcar smoothing with a 10-year window, applied at each gridpoint of the input dataset, relative to an 1850–1900 baseline. This removes the underlying global mean temperature increase, geographical patterns of global warming, and any seasonal differences. Near the endpoints, where there is insufficient data for the 10-year mean, we ensure consistent weighting by mirroring the data points. This was shown in Samset et al.[14] to have a negligible impact on the overall results, including trend estimates, even for the end years of the series. Note, however, that our chosen method will not remove decadal scale variability in regional temperature patterns.

Green's functions

We use a Green's Function (GF) calculated with the CESM1.2.1-CAM5.3 Earth System Model, monthly resolved and taking 40-year simulations with fixed sea-surface temperatures as input[18,26]. A GF, in our usage, relates an idealized increase in sea surface temperature at a given location, to resulting influences on radiation, clouds, water vapour and, ultimately, global mean surface temperature, and allows us to calculate the modulation of global mean surface temperatures resulting from a given pattern of SST variability. It is based on simulations where the SST was individually perturbed in 74 (partially overlapping) ocean patches of 80° longitude and 40° latitude. We use 2-metre surface air temperature to quantify the modulations.

GSTA modulations are calculated by multiplying Green's Function for that month with the detrended SST pattern from observations (HadCRUT5 or other series). The total modulation is the sum of the contributions from all ocean-dominated grid points. For this calculation, monthly temperature fields from the observational series have been regridded to the GF resolution (2.5° latitude, 1.9° longitude).
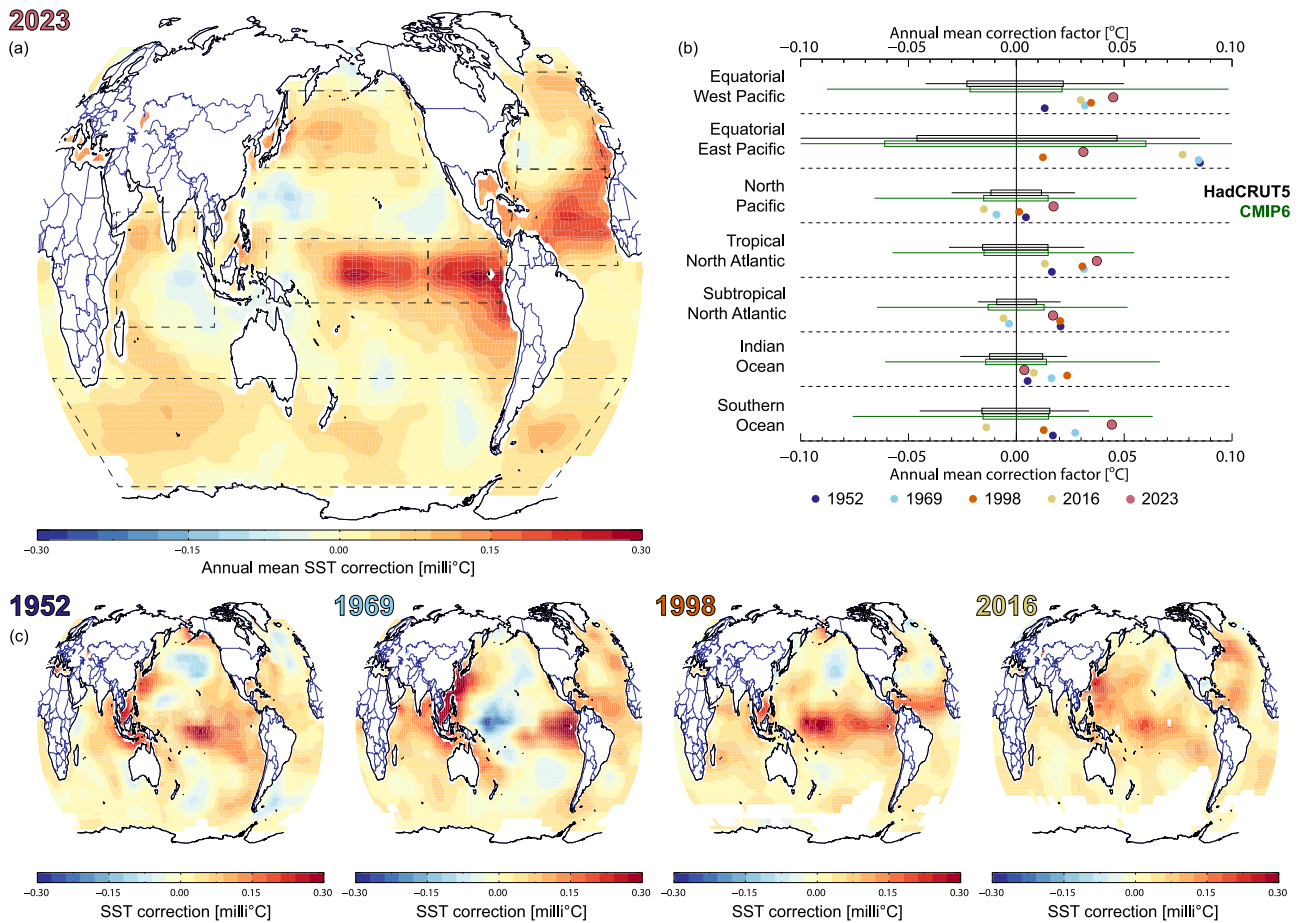
Fig. 4 | Ocean basin contributions to the 2023 temperature anomaly. SST pattern-induced corrections to the annual mean global surface temperature anomaly, for **a** 2023 and **c** the four other strongest correction years in HadCRUT5 (1950–2023). Maps show the product of Green's function and the observed SST pattern, such that the total correction (globally or regionally) is the sum of all relevant grid boxes. Note the unit (milli°C). Box-and-whiskers **b** show the mean, 5–95% and max/min ranges for five selected ocean basins, coloured dots show the strong correction years. Approximate ocean basin definitions are indicated by dashed boxes in the 2023 map.

We note that the CESM1-derived GF used here has been documented to have very similar response patterns to GFs produced with other models[16,18–20]. The applicability of equilibrium simulations to capture monthly and interannual variability has been investigated for previous publications[3,14]. While the full atmospheric response will not be realized for monthly varying SST patterns, the rapid timescales of Rossby wave train propagation and other dynamical features mean that the key features of a response do have time to develop[27,28].

Ocean basin definitions
For the ocean basin mean corrections presented in Fig. 2, we use longitude/latitude boxes shown in Table 1.

Climate model data analysis
Output from climate model simulations was analysed identically to the surface data series, including filtering using Green's Function. All simulations used were provided for the ScenarioMIP[29] CMIP6 Endorsed MIP[30], and made available to the community through the Earth System Grid Federation (ESGF). We made use of 250-year transient simulations using the CMIP6 historical (1850–2014) and Shared Socioeconomic Pathway (SSP) (2015-2100) emission datasets. Two SSPs were used (SSP1-2.6, SSP5-8.5), to extend the historical data through 2027. (The main analysis runs through 2022, but we use subsequent data to avoid the need for mirroring the endpoints). The results of Fig. 2 are

insensitive to the choice of SSP (SSP5-8.5, SSP3-7.0, SSP2-4.5, SSP1-2.6). Only monthly mean temperature data (Global Surface Air Temperature at 2 metres) was used.

CMIP6 models
The CMIP6 models used for the present study are shown in Table 2, along with the relevant model and dataset references, and the number of ensemble members.

Table 1 | Ocean basin definitions

Region	Lon		Lat	
	Min	Max	Min	Max
Equatorial West Pacific	110	240	−30	30
Equatorial East Pacific	240	280	−30	30
North Pacific	140	225	30	55
Subtropical North Atlantic	280	360	30	60
Tropical North Atlantic	280	360	0	30
Indian Ocean	40	90	−20	20
Southern Ocean	0	360	−60	−30

Unit: Degrees.

Table 2 | Climate model simulations used in the present study

Centre	Model	Ensemble members	Data reference	Documentation paper
CSIRO-ARCCSS	ACCESS-CM2	1	https://doi.org/10.22033/ESGF/CMIP6.4271	N/A
CSIRO	ACCESS-ESM1-5	30	https://doi.org/10.22033/ESGF/CMIP6.4272	[31]
AWI	AWI-ESM-1-1-LR	1	https://doi.org/10.22033/ESGF/CMIP6.9328	N/A
BCC	BCC-CSM2-MR	1	https://doi.org/10.22033/ESGF/CMIP6.2948	[32]
CAMS	CAMS-CSM1-0	1	https://doi.org/10.22033/ESGF/CMIP6.9754	[33]
CCCma	CanESM5	20	https://doi.org/10.22033/ESGF/CMIP6.3610	[34]
NCAR	CESM2	1	https://doi.org/10.22033/ESGF/CMIP6.7627	[35]
NCAR	CESM2-WACCM	1	https://doi.org/10.22033/ESGF/CMIP6.10071	[35]
CNRM-CERFACS	CNRM-CM6-1	1	https://doi.org/10.22033/ESGF/CMIP6.4066	[36]
CNRM-CERFACS	CNRM-ESM2-1	1	https://doi.org/10.22033/ESGF/CMIP6.4068	[37]
EC-Earth-Consortium	EC-Earth3	7	https://doi.org/10.22033/ESGF/CMIP6.4701	[38]
EC-Earth-Consortium	EC-Earth3-Veg	3	https://doi.org/10.22033/ESGF/CMIP6.4706	[38,39]
CAS	FGOALS-f3-L	1	https://doi.org/10.22033/ESGF/CMIP6.3355	[40]
CAS	FGOALS-g3	1	https://doi.org/10.22033/ESGF/CMIP6.3356	[41]
FIO-ESM-2-0	FIO-ESM-2-0	1	https://doi.org/10.22033/ESGF/CMIP6.9199	[42]
NOAA-GFDL	GFDL-ESM4	1	https://doi.org/10.22033/ESGF/CMIP6.8597	[43]
MOHC	HadGEM3-GC31-LL	1	https://doi.org/10.22033/ESGF/CMIP6.6109	[44]
MOHC	HadGEM3-GC31-MM	1	https://doi.org/10.22033/ESGF/CMIP6.6112	[45]
INM	INM-CM4-8	1	https://doi.org/10.22033/ESGF/CMIP6.5069	[46]
INM	INM-CM5-0	1	https://doi.org/10.22033/ESGF/CMIP6.5070	[47]
IPSL	IPSL-CM6A-LR	6	https://doi.org/10.22033/ESGF/CMIP6.13601	[48]
NIMS-KIMA	KACE-1-0-G	2	https://doi.org/10.22033/ESGF/CMIP6.8378	[49]
UA	MCM-UA-1-0	1	https://doi.org/10.22033/ESGF/CMIP6.8888	N/A
MIROC	MIROC6	1	https://doi.org/10.22033/ESGF/CMIP6.5603	[50]
MIROC	MIROC-ES2L	1	https://doi.org/10.22033/ESGF/CMIP6.5602	[51]
MPI-M	MPI-ESM1-2-HR	1	https://doi.org/10.22033/ESGF/CMIP6.6594	[52]
MPI-M	MPI-ESM1-2-LR	30	https://doi.org/10.22033/ESGF/CMIP6.6595	[53]
MRI	MRI-ESM2-0	1	https://doi.org/10.22033/ESGF/CMIP6.6842	[54]
NUIST	NESM3	1	https://doi.org/10.22033/ESGF/CMIP6.8769	[55]
NCC	NorESM2-LM	1	https://doi.org/10.22033/ESGF/CMIP6.8036	[56]
NCC	NorESM2-MM	1	https://doi.org/10.22033/ESGF/CMIP6.8040	[56]
MOHC	UKESM1-0-LL	1	https://doi.org/10.22033/ESGF/CMIP6.6113	[57]

All simulations were delivered as part of the CMIP6 exercise.

Data availability

The processed time series used for the figures in this manuscript, and the underlying analysis, are published on figshare (10.6084/m9.figshare.25721373). The CESM1 Green's Function is documented and made available at https://github.com/mzelinka/greens-function (https://doi.org/10.5281/zenodo.5514146). Surface temperature datasets are publicly available from these websites (accessed on 15.04.2024): https://www.metoffice.gov.uk/hadobs/hadcrut5/, https://data.giss.nasa.gov/gistemp/, https://www.ncei.noaa.gov/access/metadata/landing-page/bin/iso?id=gov.noaa.ncdc:C01585, https://berkeleyearth.org/data/. All climate model simulations used in this manuscript are publicly available through the ESGF (e.g. https://esgf-node.llnl.gov/projects/cmip6/).

References

1. Gulev, S. K. et al. In *Climate Change 2021: The Physical Science Basis. Contribution of Working Group I to the Sixth Assessment Report of the Intergovernmental Panel on Climate Change* (eds V. Masson-Delmotte et al.) 287–422 (Cambridge Univ. Press, 2021).
2. Forster, P. M. et al. Indicators of global climate change 2022: annual update of large-scale indicators of the state of the climate system and the human influence. *ESDD*. https://doi.org/10.5194/essd-2023-166 (2023).
3. Samset, B. H. et al. Steady global surface warming from 1973 to 2022 but increased warming rate after 1990. *Commun. Earth Environ.* https://doi.org/10.1038/s43247-023-01061-4 (2023).
4. Hansen, J. E. et al. Global warming in the pipeline. *Oxford Open Clim. Chang.* https://doi.org/10.1093/oxfclm/kgad008 (2023).
5. Hodnebrog, Ø. et al. Recent reductions in aerosol emissions have increased Earth's energy imbalance. *Commun. Earth Environ.* https://doi.org/10.1038/s43247-024-01324-8 (2024).
6. Li, Z., England, M. H. & Groeskamp, S. Recent acceleration in global ocean heat accumulation by mode and intermediate waters. *Nat. Commun.* **14**, 6888 (2023).
7. Bellouin, N. et al. Bounding global aerosol radiative forcing of climate change. *Rev. Geophys.* https://doi.org/10.1029/2019rg000660 (2020).
8. Kuhlbrodt, T., Swaminathan, R., Ceppi, P. & Wilder, T. A glimpse into the future: the 2023 ocean temperature and sea ice extremes in the context of longer-term climate change. *Bull. Am. Meteorol. Soc.* **105**, E474–E485 (2024).

9. Cheng, L. et al. New record ocean temperatures and related climate indicators in 2023. *Adv. Atmos. Sci.* **41**, 1068–1082 (2024).

10. Jiang, N. et al. Enhanced risk of record-breaking regional temperatures during the 2023-24 El Nino. *Sci. Rep.* **14**, 2521 (2024).

11. Min, S.-K. Human influence can explain the widespread exceptional warmth in 2023. *Commun. Earth Environ.* https://doi.org/10.1038/s43247-024-01391-x (2024).

12. Gettelman, A. et al. Has reducing ship emissions brought forward global warming? *Geophys. Res. Lett.* **51**, e2024GL109077 (2024).

13. Schoeberl, M. R. et al. The estimated climate impact of the Hunga Tonga-Hunga Ha'apai eruption plume. *Geophys. Res. Lett.* https://doi.org/10.1029/2023gl104634 (2023).

14. Samset, B. H. et al. Earlier emergence of a temperature response to mitigation by filtering annual variability. *Nat. Commun.* **13**, 1578 (2022).

15. Armour, K. C. et al. Sea-surface temperature pattern effects have slowed global warming and biased warming-based constraints on climate sensitivity. *Proc. Natl Acad. Sci. USA* **121**, e2312093121 (2024).

16. Bloch-Johnson, J. et al. The Green's Function Model Intercomparison Project (GFMIP) protocol. *J. Adv. Model. Earth Syst.* https://doi.org/10.1029/2023ms003700 (2024).

17. Thomson, S. I. & Vallis, G. K. Atmospheric response to SST Anomalies. Part I: background-state dependence, teleconnections, and local effects in winter. *J. Atmos. Sci.* **75**, 4107–4124 (2018).

18. Zhou, C., Zelinka, M. D. & Klein, S. A. Analyzing the dependence of global cloud feedback on the spatial pattern of sea surface temperature change with a Green's function approach. *J. Adv. Model. Earth Syst.* **9**, 2174–2189 (2017).

19. Dong, Y., Proistosescu, C., Armour, K. C. & Battisti, D. S. Attributing historical and future evolution of radiative feedbacks to regional warming patterns using a Green's function approach: the preeminence of the Western Pacific. *J. Clim.* **32**, 5471–5491 (2019).

20. Zhang, B., Zhao, M. & Tan, Z. Using a Green's function approach to diagnose the pattern effect in GFDL AM4 and CM4. *J. Clim.* **36**, 1105–1124 (2023).

21. Morice, C. P. et al. An updated assessment of near-surface temperature change from 1850: the HadCRUT5 data set. *J. Geophys. Res. Atmos.* https://doi.org/10.1029/2019jd032361 (2021).

22. Forster, P. M. et al. Indicators of global climate change 2023: annual update of key indicators of the state of the climate system and human influence. *Earth Syst. Sci. Data* **16**, 2625–2658 (2024).

23. Lenssen, N. J. L. et al. Improvements in the uncertainty model in the Goddard Institute for Space Studies Surface Temperature (GISTEMP) analysis. *J. Geophys. Res. Atmos.* https://doi.org/10.1029/2018jd029522 (2019).

24. Team, G. GISS Surface Temperature Analysis (GISTEMP), version 4 https://data.giss.nasa.gov/gistemp/ (2023).

25. Rohde, R. A. & Hausfather, Z. The Berkeley earth land/ocean temperature record. *Earth Syst. Sci. Data* **12**, 3469–3479 (2020).

26. Zhou, C., Lu, J., Hu, Y. & Zelinka, M. D. Responses of the Hadley circulation to regional sea surface temperature changes. *J. Clim.* **33**, 429–441 (2020).

27. Sardeshmukh, P. D. & Hoskins, B. J. The generation of global rotational flow by steady idealized tropical divergence. *J. Atmos. Sci.* **45**, 1228–1251 (1988).

28. Stjern, C. W. et al. The time scales of climate responses to carbon dioxide and aerosols. *J. Clim.* **36**, 3537–3551 (2023).

29. O'Neill, B. C. et al. The Scenario Model Intercomparison Project (ScenarioMIP) for CMIP6. *Geosci. Model Dev.* **9**, 3461–3482 (2016).

30. Eyring, V. et al. Overview of the Coupled Model Intercomparison Project Phase 6 (CMIP6) experimental design and organization. *Geosci. Model Dev.* **9**, 1937–1958 (2016).

31. Ziehn, T. et al. The Australian Earth System Model: ACCESS-ESM1.5. *J. South. Hemisph. Earth Syst. Sci.* **70**, 193–214 (2020).

32. Wu, T. et al. The Beijing Climate Center Climate System Model (BCC-CSM): the main progress from CMIP5 to CMIP6. *Geosci. Model Dev.* **12**, 1573–1600 (2019).

33. RONG, X.-Y. et al. Introduction of CAMS-CSM model and its participation in CMIP6. *Clim. Change Res.* **15**, 540–544 (2019).

34. Swart, N. C. et al. The Canadian Earth System Model version 5 (CanESM5.0.3). *Geosci. Model Dev.* **12**, 4823–4873 (2019).

35. Danabasoglu, G. et al. The Community Earth System Model Version 2 (CESM2). *J. Adv. Model. Earth Syst.* https://doi.org/10.1029/2019ms001916 (2020).

36. Voldoire, A. et al. Evaluation of CMIP6 DECK experiments with CNRM-CM6-1. *J. Adv. Model. Earth Syst.* **11**, 2177–2213 (2019).

37. Séférian, R. et al. Evaluation of CNRM Earth System Model, CNRM-ESM2-1: role of earth system processes in present-day and future climate. *J. Adv. Model. Earth Syst.* **11**, 4182–4227 (2019).

38. Döscher, R. et al. The EC-Earth3 earth system model for the Coupled Model Intercomparison Project 6. *Geosci. Model Dev.* **15**, 2973–3020 (2022).

39. Wyser, K. et al. On the increased climate sensitivity in the EC-Earth model from CMIP5 to CMIP6. *Geosci. Model Dev.* **13**, 3465–3474 (2020).

40. He, B. et al. CAS FGOALS-f3-L model datasets for CMIP6 historical atmospheric model intercomparison project simulation. *Adv. Atmos. Sci.* **36**, 771–778 (2019).

41. Li, L. et al. The Flexible Global Ocean-Atmosphere-Land System Model Grid-Point Version 3 (FGOALS-g3): description and evaluation. *J. Adv. Model. Earth Syst.* https://doi.org/10.1029/2019ms002012 (2020).

42. Bao, Y., Song, Z. & Qiao, F. FIO-ESM version 2.0: model description and evaluation. *J. Geophys. Res. Oceans* https://doi.org/10.1029/2019jc016036 (2020).

43. Dunne, J. P. et al. The GFDL Earth System Model Version 4.1 (GFDL-ESM 4.1): overall coupled model description and simulation characteristics. *J. Adv. Model. Earth Syst.* https://doi.org/10.1029/2019ms002015 (2020).

44. Kuhlbrodt, T. et al. The low-resolution version of HadGEM3 GC3.1: development and evaluation for global climate. *J. Adv. Model Earth Syst.* **10**, 2865–2888 (2018).

45. Andrews, M. B. et al. Historical simulations with HadGEM3-GC3.1 for CMIP6. *J. Adv. Model. Earth Syst.* https://doi.org/10.1029/2019ms001995 (2020).

46. Volodin, E. M., Dianskii, N. A. & Gusev, A. V. Simulating present-day climate with the INMCM4.0 coupled model of the atmospheric and oceanic general circulations. *Izv. Atmos. Ocean. Phys.* **46**, 414–431 (2010).

47. Volodin, E. M. et al. Simulation of the present-day climate with the climate model INMCM5. *Clim. Dyn.* **49**, 3715–3734 (2017).

48. Bonnet, R. et al. Presentation and evaluation of the IPSL-CM6A-LR ensemble of extended historical simulations. *J. Adv. Model. Earth Syst.* https://doi.org/10.1029/2021ms002565 (2021).

49. Lee, J. et al. Evaluation of the Korea Meteorological Administration Advanced Community Earth-System model (K-ACE). *Asia-Pac. J. Atmos. Sci.* **56**, 381–395 (2019).

50. Tatebe, H. et al. Description and basic evaluation of simulated mean state, internal variability, and climate sensitivity in MIROC6. *Geosci. Model Dev.* **12**, 2727–2765 (2019).

51. Hajima, T. et al. Development of the MIROC-ES2L Earth system model and the evaluation of biogeochemical processes and feedbacks. *Geosci. Model Dev.* **13**, 2197–2244 (2020).

52. Müller, W. A. et al. A higher-resolution version of the Max Planck Institute Earth System Model (MPI-ESM1.2-HR). *J. Adv. Model. Earth Syst.* **10**, 1383–1413 (2018).

53. Olonscheck, D. et al. The New Max Planck Institute Grand Ensemble with CMIP6 forcing and high-frequency model output. *J. Adv. Model. Earth Syst.* https://doi.org/10.1029/2023ms003790 (2023).

54. Yukimoto, S. et al. The Meteorological Research Institute Earth System Model version 2.0, MRI-ESM2.0: description and basic evaluation of the physical component. *J. Meteorol. Soc. Jpn. Ser. II* **97**, 931–965 (2019).
55. Cao, J. et al. THE NUIST Earth System Model (NESM) version 3: description and preliminary evaluation. *Geosci. Model Dev.* **11**, 2975–2993 (2018).
56. Seland, Ø. et al. Overview of the Norwegian Earth System Model (NorESM2) and key climate response of CMIP6 DECK, historical, and scenario simulations. *Geosci. Model Dev.* **13**, 6165–6200 (2020).
57. Sellar, A. A. et al. UKESM1: description and evaluation of the U.K. Earth System Model. *J. Adv. Model. Earth Syst.* **11**, 4513–4558 (2019).

Author contributions

B.H.S. conceived and designed the study, performed the analysis, and wrote the paper. J.S.F., M.T.L. and L.J.W. contributed to shaping the conclusions, discussing and testing the methods, and writing the paper.

Competing interests

The authors declare no competing interests.

Additional information

Supplementary information The online version contains supplementary material available at https://doi.org/10.1038/s43247-024-01637-8.

Correspondence and requests for materials should be addressed to Bjørn H. Samset.

Peer review information *Communications Earth & Environment* thanks Dirk Olonscheck and the other, anonymous, reviewer(s) for their contribution to the peer review of this work. Primary Handling Editors: Sylvia Sullivan and Alireza Bahadori. A peer review file is available.

Reprints and permissions information is available at http://www.nature.com/reprints

Publisher's note Springer Nature remains neutral with regard to jurisdictional claims in published maps and institutional affiliations.